DOI: 10.1002/eqe.3803

RESEARCH ARTICLE

Damping-dependent correlations between response spectral ordinates

Alan Poulos | Eduardo Miranda

Department of Civil and Environmental Engineering, Stanford University, Stanford, CA, USA

Correspondence
Alan Poulos, Department of Civil and Environmental Engineering, Stanford University, CA 94305, USA.
Email: apoulos@stanford.edu

Abstract

Correlations between response spectral ordinates at different periods are used in several seismic hazard computations, such as for the construction of conditional mean spectra and conditional spectra. Conventionally, these correlations have been computed and reported only for a damping ratio of 5%; however, structures may have damping ratios substantially lower or higher than 5% and therefore, in those cases, it is necessary to know the correlations of spectral ordinates at different periods but having the same damping ratios that are different than 5%, correlations of spectral ordinates at the same period but having different damping ratios, and the generalized case of correlation between response spectral ordinates of two oscillators having different damping ratios and different periods. This work computes such damping-dependent correlations by using the NGA-West2 ground motion database. In general, it is found that correlations increase as the damping ratio of any of the two spectral ordinates increases and as the ratio of periods of vibration of the two oscillators departs from one. A nonlinear regression model is fitted to the resulting damping-dependent correlations to simplify future computations. Finally, the use of the new damping-dependent correlations is illustrated by computing example conditional spectra for damping ratios differing from 5%. The results show that using 5%-damped correlations for the construction of condition mean spectra, overestimates spectral ordinates for damping ratios lower than 5% and underestimates spectral ordinates for damping ratios higher than 5%.

KEYWORDS:
correlation, spectral ordinates, damping ratios, conditional spectra

1 | INTRODUCTION

In earthquake engineering, ground motion intensity is usually characterized by a 5%-damped linear elastic response spectrum. Most earthquake-resistant design codes [1] and ground motion models (GMMs) [2,3,4] use this intensity measure. However, there are several cases in which spectral accelerations for damping ratios other than 5% are important. For example, modal damping ratios of first translational modes of high-rise buildings are significantly lower than 5% [5,6,7], whereas spectral ordinates for damping ratios higher than 5% are of interest for building with seismic isolation systems and energy dissipation devices [1], for many non-slender low-rise buildings [7], and for seismic demand estimations on some higher modes of vibrations of buildings [8].

Although some GMMs have been developed to directly estimate spectral accelerations for damping ratios other than 5%[9,10], most studies have developed models for multiplicative factors that scale 5%-damped spectral accelerations to spectral accelerations for other damping ratios[11,12,13], which are usually referred to as damping modification factors or damping scaling factors. Most recent models of these damping modification factors depend on the period of vibration[12] and in some cases also on some common predictor variables of GMMs (e.g., earthquake magnitude and source-to-site distance)[13]. These models can be used to adjust the logarithmic mean spectral acceleration given by GMMs and in some cases also its logarithmic standard deviation[13]. Since spectral accelerations are usually assumed to follow a lognormal probability distribution, these two parameters provide a complete description of the marginal distribution of spectral accelerations for any value of damping.

However, there are several applications where the joint probability distribution of spectral accelerations at different periods of vibration is needed, such as for vector-valued probabilistic seismic hazard analysis[14], the construction of conditional spectra[15] or conditional mean spectra[16], or the simulation of individual realizations of response spectra for a given earthquake scenario[15,17]. Since the joint distribution of logarithmic spectral accelerations has been found to be well represented by a multivariate normal distribution[18], the only additional information required to define this distribution is the correlation between logarithmic spectral accelerations at different periods. Several models have already been developed for these correlations[17,19,20,21,22,23]; however, to the best of the authors' knowledge, no model has been developed for correlations between spectral accelerations of damping ratios other than 5%.

This work studies the correlations between spectral accelerations of different damping ratios. The correlations are computed empirically using a large database of ground motion from shallow crustal earthquakes in active tectonic regimes. A nonlinear regression model is then calibrated using the empirically-computed correlations, which, in addition to having the two periods of vibration as input used in previous models, it now also depends on the damping ratios of both oscillators for which the spectral acceleration ordinates are computed. Finally, the estimated correlations are used to construct conditional spectra for an example earthquake scenario to study the effects of using non-5%-damped correlations.

2 | METHODS

2.1 | Ground motion database

The correlations of this study were computed using the NGA-West2 ground motions database developed by the Pacific Earthquake Engineering Research Center, which consists of recordings from shallow crustal earthquakes in active tectonic regions[24]. For comparison purposes, this study uses the same records as those used by Baker and Bradley[22], which were defined using the record selection criteria of Chiou and Youngs[4]. Moreover, to focus on ground motions of engineering significance, only records from earthquakes of magnitude greater than or equal to 5 and source-to-site distances shorter than 100 km were considered, although ground motions recorded at distances longer than 100 km were also used to compute between event residuals. Spectral accelerations were only computed up to the maximum usable period of each record indicated in the NGA-West2 database.

The distribution of magnitudes and source-to-site distances of the selected ground motions is presented in Figure 1. A total of 4,234 records were used, with 1,984 of them having source-to-site distances shorter than 100 km. Most records correspond to earthquakes with reverse and strike-slip focal mechanism, which represent 57.5% and 41.4% of the records, respectively, and only 1.1% are from earthquakes occurring in normal faults.

2.2 | Correlation estimation

Most GMMs assume that spectral accelerations have the following mixed-effects form:

$$\ln Sa(T,\xi) = \mu_{\ln Sa}(T,\xi) + \delta B(T,\xi) + \delta W(T,\xi) \tag{1}$$

where $\ln Sa$ is the logarithm of the spectral acceleration measured at a given site; $\mu_{\ln Sa}$ is the logarithmic mean spectral acceleration given by a GMM, which depends on several predictive variables, such as earthquake magnitude, source-to-site distance, and local site conditions. The difference between the measured and predicted logarithmic standard deviation is separated in the between-event residual δB and the within-event residual δW, which are both assumed to be normally distributed random variables with zero mean and standard deviations of τ and ϕ, respectively, whose values are also given by the GMM. The sum of

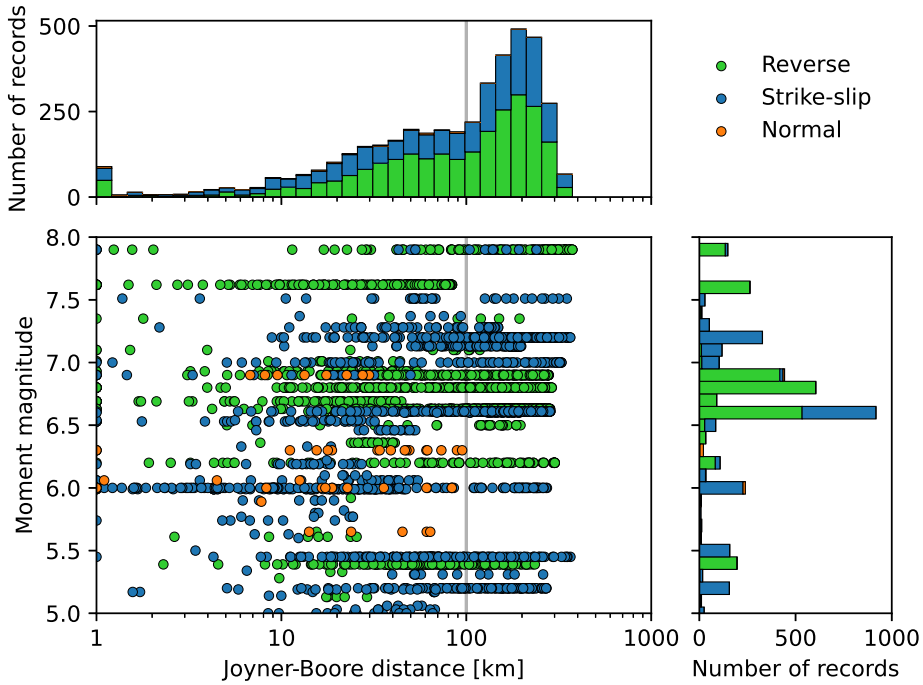

FIGURE 1 Moment magnitude and Joyner-Boore distance distribution of the ground motion records used in this study. In this figure, records with distances shorter than 1 km are lumped at 1 km.

the two residuals correspond is the total residual, $\delta = \delta B + \delta W$, which has a standard deviation of $\sigma_{\ln Sa} = \sqrt{\tau^2 + \phi^2}$ because δB and δW are assumed to be independent random variables.

This study uses the GMM developed by Chiou and Youngs[4] to compute the logarithmic mean and standard deviations of Equation (1) for a 5% damping ratio, although three other GMMs[2,3,25] were also used to evaluate their effect on the empirically-computed correlations. These values are then transformed to other damping ratios using the damping scaling factor (DSF) developed by Rezaeian et al.[13]:

$$\mu_{\ln Sa}(T,\xi) = \mu_{\ln Sa_{5\%}}(T) + \mu_{\ln DSF}(T,\xi) \tag{2}$$

$$\sigma_{\ln Sa}(T,\xi) = \sqrt{\sigma^2_{\ln Sa_{5\%}}(T) + \sigma^2_{\ln DSF}(T,\xi) + 2\sigma_{\ln Sa_{5\%}}(T)\sigma_{\ln DSF}(T,\xi)\rho_{\ln Sa_{5\%},\ln DSF}(T,\xi)} \tag{3}$$

where $\mu_{\ln Sa}(T,\xi)$ and $\sigma_{\ln Sa}(T,\xi)$ are, respectively, the mean and standard deviation of the logarithm of spectral acceleration for an arbitrary damping ratio ξ; $\mu_{\ln Sa_{5\%}}(T)$ and $\sigma_{\ln Sa_{5\%}}(T)$ are, respectively, the mean and standard deviation of the logarithm of the 5%-damped spectral acceleration, which is given by the GMM; $\mu_{\ln DSF}(T,\xi)$ is the logarithmic mean DSF used to transform from a damping ratio of 5% to ξ, which also corresponds to the median DSF because its distribution is assumed to be lognormal[13]; $\sigma_{\ln Sa_{5\%}}(T,\xi)$ is the logarithmic standard deviation of DSF; and $\rho_{\ln Sa_{5\%},\ln DSF}(T,\xi)$ is the correlation between the logarithm of the 5%-damped spectral acceleration and the logarithm of DSF for a damping ratio of ξ, which was obtained from Rezaeian et al.[26].

The model developed by Rezaeian et al.[13] only modifies the standard deviation of the total residuals; thus, the modification of the standard deviations of between-event and within-event residuals were assumed to be proportional to the modification of the standard deviation of total residuals:

$$\tau(T,\xi) = \tau_{5\%}(T)\frac{\sigma_{\ln Sa}(T,\xi)}{\sigma_{\ln Sa_{5\%}}(T)} \tag{4}$$

$$\phi(T,\xi) = \phi_{5\%}(T)\frac{\sigma_{\ln Sa}(T,\xi)}{\sigma_{\ln Sa_{5\%}}(T)} \tag{5}$$

where $\tau_{5\%}(T)$ and $\phi_{5\%}(T)$ are the standard deviations of 5%-damped between-event and within-event residuals, respectively.

Once the logarithmic means and standard deviations are computed, the between-event residual of each earthquake can be computed using a maximum likelihood estimate given by:

$$\delta B(T,\xi) = \frac{\sum_{i=1}^{n} \frac{\delta_i(T,\xi)}{\phi_i^2(T,\xi)}}{\frac{1}{\tau^2(T,\xi)} + \sum_{i=1}^{n} \frac{1}{\phi_i^2(T,\xi)}} \tag{6}$$

where n is the number of recordings of the earthquake; δ_i is the total residual for the i-th recording of the earthquake, which can be computed using Equation (1); ϕ_i is the standard deviation of the within-event residual for the i-th recording of the earthquake; and τ is the standard deviation of the between-event residual. This is a slight modification of the method proposed by Abrahamson and Youngs[27], which accounts for the variation between sites of the within-event standard deviation within the same earthquake. The within-event residuals of the earthquake, δW_i, are then computed as:

$$\delta W_i(T,\xi) = \delta_i(T,\xi) - \delta B(T,\xi) \tag{7}$$

This work studies the general case of correlation coefficient between total residuals of logarithmic spectral acceleration (δ) of two oscillators having different damping ratios and different periods, which can be computed by combining the correlations for between-event and within-event residuals. The correlation between residuals for period and damping ratio pairs of (T_1, ξ_1) and (T_2, ξ_2) is:

$$\rho(T_1,\xi_1,T_2,\xi_2) = \frac{\tau(T_1,\xi_1)\tau(T_2,\xi_2)\rho_B(T_1,\xi_1,T_2,\xi_2) + \phi(T_1,\xi_1)\phi(T_2,\xi_2)\rho_W(T_1,\xi_1,T_2,\xi_2)}{\sigma_{\ln Sa}(T_1,\xi_1)\sigma_{\ln Sa}(T_2,\xi_2)} \tag{8}$$

where $\rho_B(T_1,\xi_1,T_2,\xi_2)$ is the correlation coefficient of the between-event residuals, and $\rho_W(T_1,\xi_1,T_2,\xi_2)$ is the correlation coefficient of the within-event residuals. These two correlations are computed as the Pearson correlation coefficient for between-event and within-event residuals, respectively. Correlation coefficients were computed using the previously described method for all possible combinations of periods and damping ratios of the NGA-West2 flatfiles, which consist of 105 periods between 0.01 s and 10 s and 11 damping ratios with the following values: 0.5%, 1%, 2%, 3%, 5%, 7%, 10%, 15%, 20%, 25%, and 30%. Records with a maximum usable period lower than $\max\{T_1, T_2\}$ were not used to compute correlations, which led to the set of records used being period-dependent. The case where the two periods are different, but both have a 5% damping ratio as considered in previous models, or cases where the periods of the two oscillators are different but both have the same damping ratio which is different than 5%, or where the period is the same in both oscillators but their damping ratios are different are all particular cases of the generalized correlations previously described.

2.3 | Nonlinear regression model

To simplify the use of the empirically-computed correlations, such as for constructing conditional spectra or for simulating individual realizations of response spectral ordinates corresponding to specific modal periods and specific modal damping ratios, a nonlinear regression model was fitted to the difference between the computed correlations and the 5%-damped correlations. The correlation between total residuals for different periods and damping ratios can be rewritten as:

$$\rho(T_1,\xi_1,T_2,\xi_2) = \rho_{5\%}(T_1,T_2) + \Delta(T_1,\xi_1,T_2,\xi_2) \tag{9}$$

where $\rho_{5\%}(T_1,T_2)$ is the correlation of residuals of spectral accelerations of two 5%-damped oscillators having periods of vibration T_1 and T_2, and $\Delta(T_1,\xi_1,T_2,\xi_2)$ is the difference between the correlations for the general case of residuals of spectral accelerations of two oscillators that have different damping ratios and those when both have a damping ratio of 5%. A nonlinear regression was conducted by considering the following functional form for this difference in correlations:

$$\Delta(T_1,\xi_1,T_2,\xi_2) = A(T_1,T_2)x_1^2 + A(T_2,T_1)x_2^2 + B(T_1,T_2)x_1 + B(T_2,T_1)x_2 + C(T_1,T_2)x_1x_2 \tag{10}$$

where A, B, and C are regression coefficients that depend on the periods of vibration of the two oscillators for which the spectral accelerations are being computed; and x_1 and x_2 depend on the corresponding damping ratios of the two oscillators:

$$x_1 = \ln(\xi_1/0.05) \tag{11}$$

$$x_2 = \ln(\xi_2/0.05) \tag{12}$$

Note that this functional form already satisfies the condition that when both oscillators have a damping ratio of 5%, no modification is made to the 5%-damped correlations, that is:

$$\rho(T_1, 0.05, T_2, 0.05) = \rho_{5\%}(T_1, T_2) \tag{13}$$

Moreover, the symmetry of correlation coefficients leads to C being a symmetric function:

$$\rho(T_1, \xi_1, T_2, \xi_2) = \rho(T_2, \xi_2, T_1, \xi_1) \quad \Rightarrow \quad C(T_1, T_2) = C(T_2, T_1) \tag{14}$$

Thus, the matrix of regression coefficients with values of C must be symmetric. Furthermore, correlations between the same period and damping pair must be equal to one, which leads to additional constraints on the diagonal of the matrices of regression coefficients:

$$\rho(T, \xi, T, \xi) = 1 \quad \Rightarrow \quad B(T, T) = 0 \ \wedge \ C(T, T) = -2A(T, T) \tag{15}$$

The coefficients of Equation (10) were obtained by conducting a nonlinear regression analysis for each period combination using the Levenberg–Marquardt algorithm[28].

3 | RESULTS

3.1 | Correlations for 5% damping

The empirically-computed correlations for 5%-damped spectral accelerations are shown in Figure 2 for the particular case in which one of the periods (T_2) is fixed at 0.1 and when fixed at 2 s and the other period (T_1) is varied. The figure compares the correlations computed in this study with those computed in four previous works: (1) the correlations computed by Baker and Jayaram[20] (not their predictive equations) using the GMM developed by Chiou and Youngs[29] and the NGA ground motion database; (2) the correlations from the electronic supplement of Abrahamson et al.[25] based on that GMM and the NGA-West2 database; (3) the correlations computed by Akkar et al.[21] using European ground motions; and (4) the correlations computed by Baker and Bradley[22] using the NGA-West2 database. In general, the correlations computed in this study are similar to those of previous works, especially to the correlations computed by Baker and Jayaram[20], which are usually within the 95% confidence bands of the computed correlations. The most significant difference is found when comparing with the correlations computed by Akkar et al.,[21] which may be attributed to its use of a completely different ground motion database. It should be noted that some differences also exist with the correlations computed by Baker and Bradley[22], even though they used the same ground motion records and the same method to compute correlations as the one that is used in this work. We were initially surprised by these differences, however, after studying their Matlab source code[30], we concluded that the difference occurs due to an incorrect set of values used for the $Z_{1.0}$ variable that is required in the Chiou and Youngs GMM[4], which corresponds to the depth to the shear-wave velocity horizon of 1 km/s. Their updated code now produces almost identical correlation values to the ones computed in this study[30].

The impact of two modeling choices required to compute these correlations between two spectral ordinates was also studied when using 5%-damped correlations: (a) the use of a specific GMM to compute the residual and standard deviations of Equation (1), and (b) the set of ground motion records used. Figure 3a illustrates the effect of the selected GMM by comparing the correlations obtained using the ground motion set described in Section 2.1 in combination with the GMM developed by Chiou and Youngs[4] with those computed using the same set of ground motions but now using GMMs developed by Boore et al.[2], by Campbell and Bozorgnia[3], and by Abrahamson et al.[25] As shown in this figure, the GMM used for computing the residuals has a negligible effects when periods T_1 and T_2 are close to each other and a moderate effect when these two periods differ more

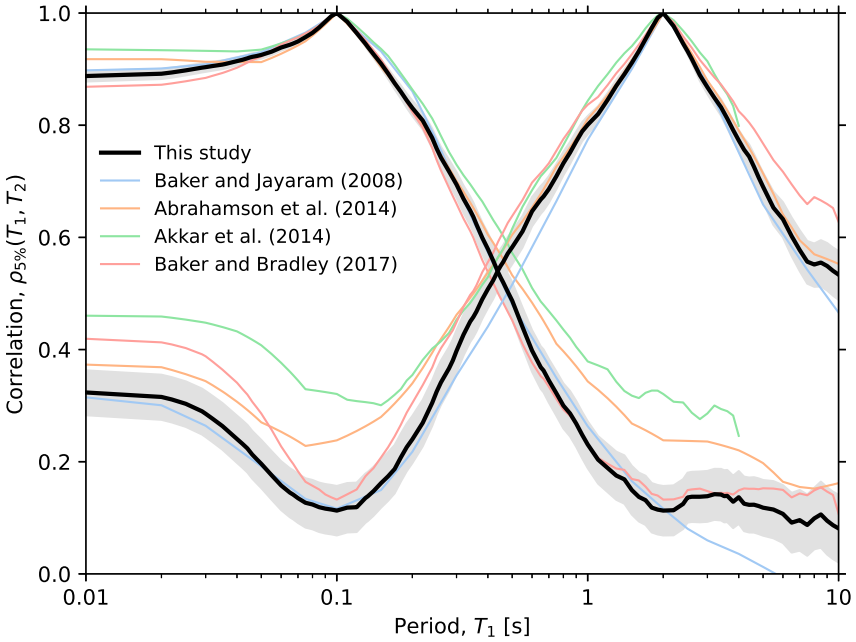

FIGURE 2 Correlations of 5%-damped spectral accelerations when the period of one of the oscillators is fixed at $T_2 = 0.1$ s or $T_2 = 2$ s and the other period T_1 is varied between 0.01 and 10 s, compared with the correlations from previous works. Shaded areas correspond to 95% pointwise confidence bands of the computed correlations.

from each other, with the maximum difference in the correlations shown in Figure 3a being approximately 0.13, which occurs for $T_1 = 10$ s and $T_2 = 0.5$ s. Thus, using different GMM does not necessarily yield nearly identical correlations as previously reported[17], although it may be reasonable to neglect the dependence on the GMM for most applications given that correlations are usually less important than means and standard deviations of spectral accelerations.

Figure 3b compares correlations computed with three different sets of ground motion records, each of which corresponds to the set that was used to develop the associated GMMs[2,3,4] that are within the magnitude and source-to-site distance constraints considered in this study (i.e., magnitudes greater than 5 and distances shorter than 100 km). The correlations shown in this figure using the three different sets of ground motion records were computed using the same GMM developed by Chiou and Youngs[4]. The differences between the different ground motion sets are also negligible when periods T_1 and T_2 are close to each other and moderate as they become farther apart but in general the effect of the ground motion set is smaller than the differences that occur when using the same ground motion set but different GMMs. It is important to note that, although the three different sets of ground motion records considered in this analysis are different from each other, they are all subsets of the NGA-West2 database. For example, approximately 69% of the records used by Chiou and Young[4] with magnitude greater than or equal to 5 and source-to-site distance shorter than 100 km were also used by the other two GMMs[2,3]. Ground motion sets that originate from different databases could lead to differences that are more significant than those presented in Figure 3b.

3.2 | Correlations for the same damping ratios

Figure 4 presents the correlations of spectral ordinates resulting for cases in which both oscillators have the same damping ratios (i.e., $\xi_1 = \xi_2$), which, for the correlations shown in this figure, are set to 1%, 5%, and 20%. As shown in this figure, for any pair of periods that are different from each other (T_1, T_2), regardless of how close or distant are the periods, the resulting correlations increase as the damping ratio increases. Moreover, the difference in correlations increase very rapidly as soon as the periods T_1 and T_2 start to depart from each other, hence making the differences in correlation significant even when the two periods are still fairly similar to each other. Figure 4 also presents 95% confidence pointwise confidence bands for the computed correlations, which originate because, despite having used a ground motion set of almost two thousand records, the effect of the sample size becomes clearly noticeable as the level of correlation decreases which leads not only to wider confidence bands but

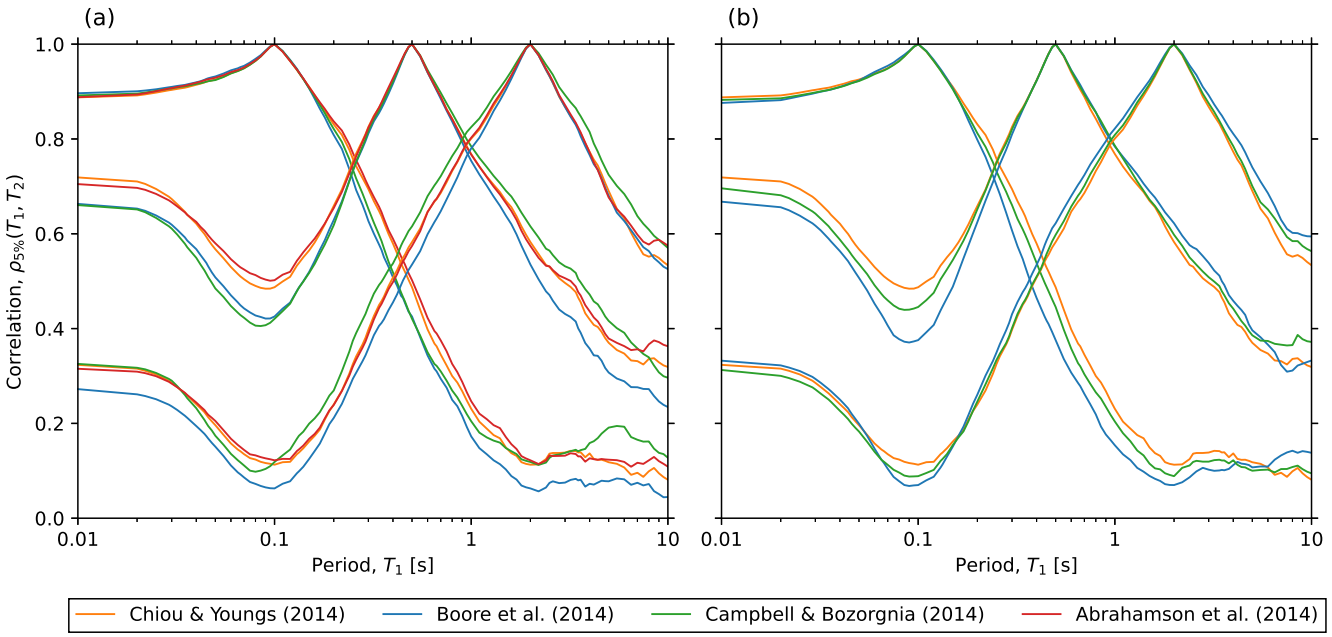

FIGURE 3 Correlations of 5%-damped spectral accelerations computed using (a) different GMMs and (b) different sets of ground motion records. One of periods is fixed at $T_2 = 0.1$ s, $T_2 = 0.5$ s, and $T_2 = 2$ s.

also less smooth correlation estimates. Moreover, the number of usable records decreases as the period of vibration increases, which starts to become noticeable for periods longer than approximately 2 s.

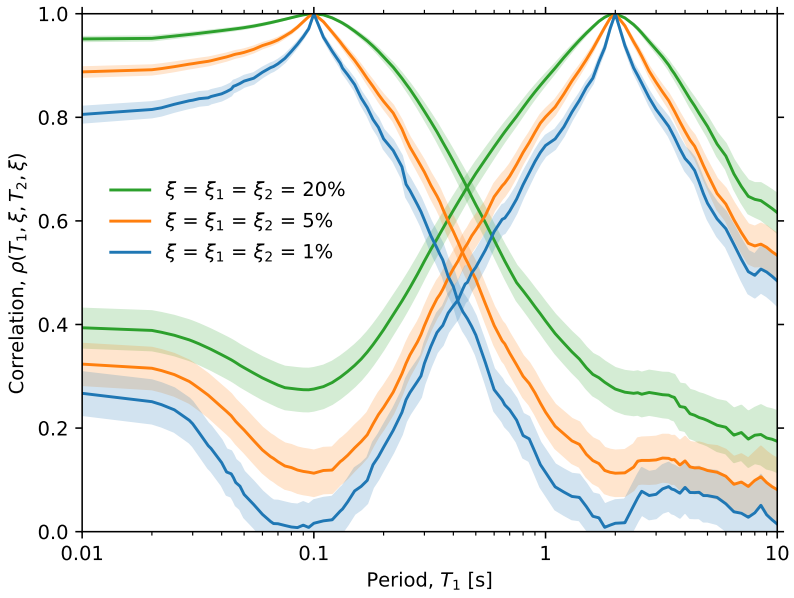

FIGURE 4 Correlations of spectral acceleration ordinates for cases in which the two oscillators have the same damping ratios. Shaded areas represent 95% pointwise confidence bands of the computed correlations.

The difference between correlations of spectral ordinates for all damping ratios and the correlations of spectral ordinates computed with 5% damping is presented in Figure 5 for the case when one period is fixed at $T_2 = 1$ s and T_1 is varied between

0.01 and 10 s. As expected, the correlations increase with increasing damping ratio throughout the range of damping ratios and for every period T_1. The differences in correlation are significant, with the correlation for 30% and 0.5% differing by a maximum of approximately 0.4 when $T_1 = 0.085$ s. In general, the differences in correlation increase as the periods separate from each other, although when T_1 becomes smaller than roughly 0.08 s, the differences start to diminish because the correlations start to increase.

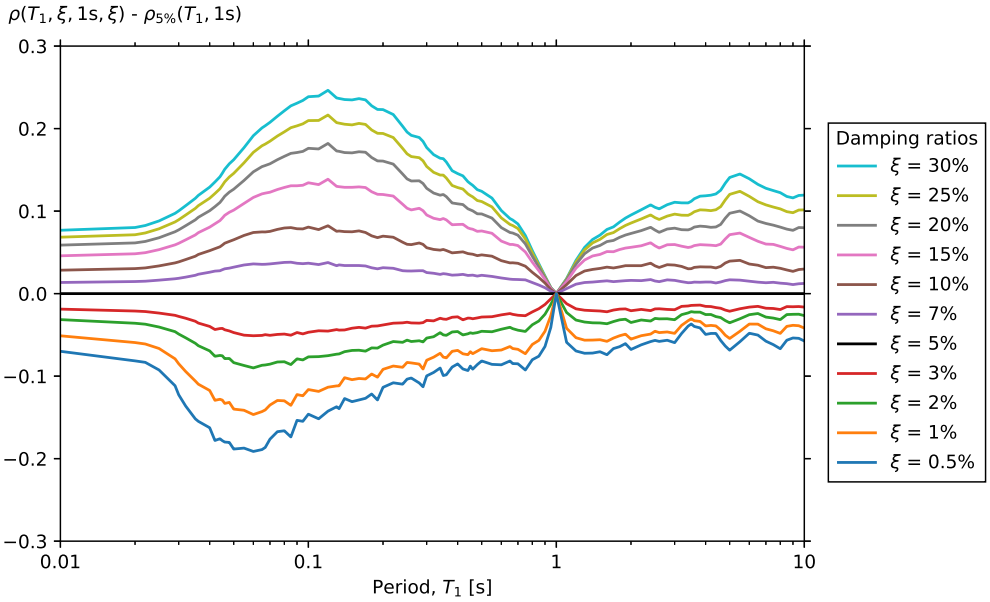

FIGURE 5 Differences between correlations of different damping ratios and the 5%-damped correlations when one of the periods is fixed at $T_2 = 1$ s.

3.3 | Correlations for different damping ratios

The general case consists of the correlation of spectral accelerations of oscillators having both different periods and different damping ratios. The surfaces of Figure 6 show the correlation of response spectral ordinates as a function of the damping ratio of the oscillators for the particular cases when the first period is $T_1 = 1$ s and the second period has values of 0.1, 0.3, 1, and 3 s. The case in which both oscillators have a damping ratio of 5%, which is the only case studied in previous works, corresponds to only a single point on each of these surfaces, represented by black circles in Figure 6. When the periods depart from each other, the correlations generally increase if any of the two damping ratios increase, which is similar to the trend found for the correlation between response spectral accelerations of both oscillators having the same damping ratio (Figure 4). However, when both periods are the same (Figure 6c), the correlations decrease as the two damping ratios become more distant from each other, regardless of whether the damping ratios of the oscillators increase or decrease.

Correlations between the peak ground velocity (PGV) and spectral accelerations of different periods and various levels of damping ratios were also computed and are shown in Figure 7. Similar to the correlations between two spectral acceleration ordinates, the correlations between PGV and spectral acceleration ordinates also increase as the damping ratio increases. For example, the correlation between PGV and the spectral acceleration at 0.1 s ranges from approximately 0.29 to 0.58 for damping ratios of 0.5% and 30%, respectively. These values are approximately 29% lower and 41% higher than the correlations between PGV and the 5%-damped spectral acceleration at 0.1 s.

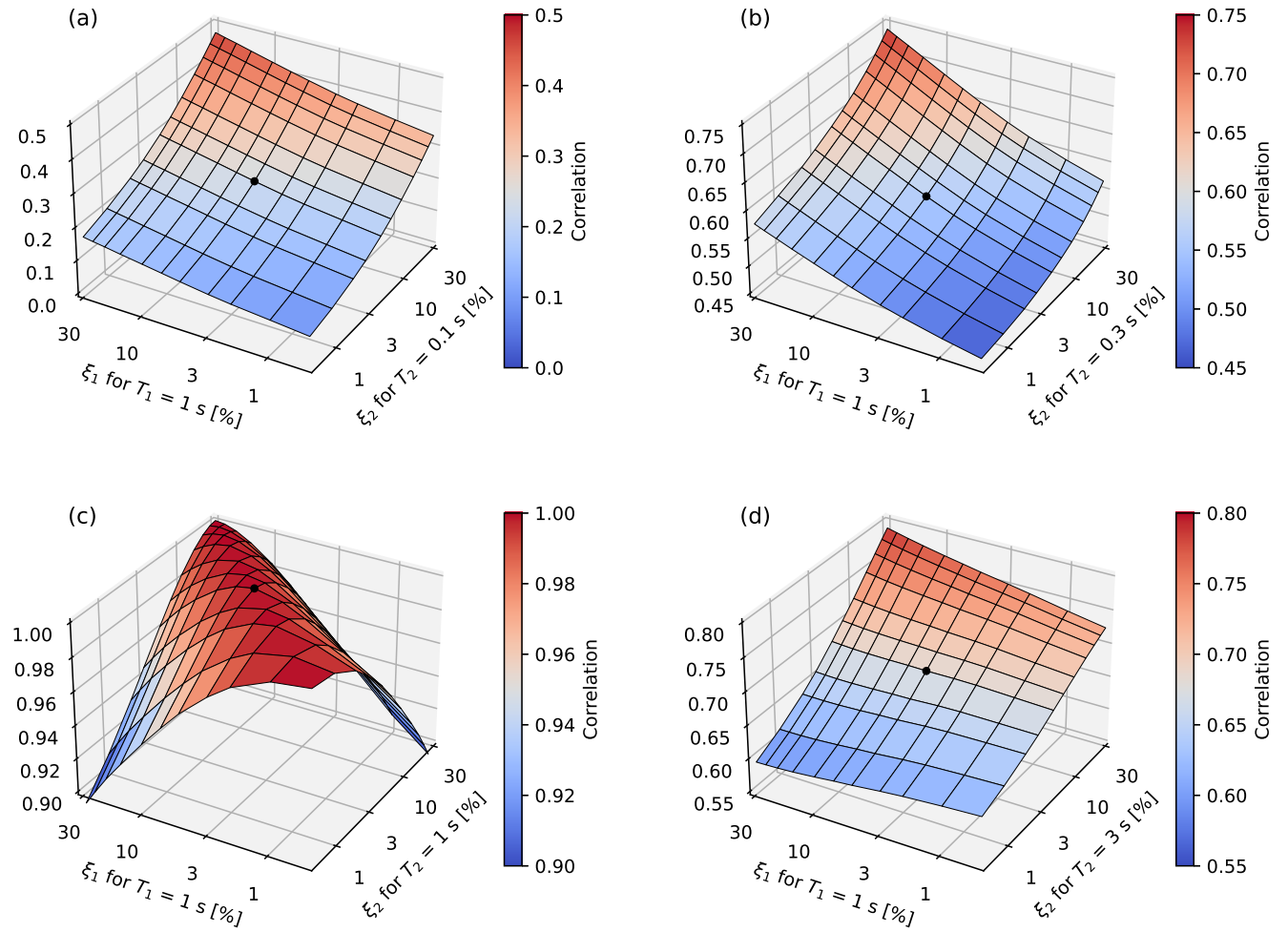

FIGURE 6 Correlations between response spectral ordinates at $T_1 = 1$ s and the response spectral ordinates at: (a) $T_2 = 0.1$ s, (b) $T_2 = 0.3$ s, (c) $T_2 = 1$ s, and (d) $T_2 = 3$ s, as a function of the damping ratios in the two oscillators. The black point on each surface corresponds to the case when both oscillators have 5% damping.

3.4 | Regression model

The regression model of Equation (10) was fitted for all pairs of periods (T_1, T_2) and the resulting coefficients were stored in matrices A, B, and $C \in \mathbb{R}^{105x105}$. Computing correlations using the regression model also requires the 5%-damped correlations of Equation (9). Tables for $\rho_{5\%}$, A, B, and C are presented in the supporting information to this article.

The differences between the correlations computed directly from the data and the correlations from the regression model are presented in Figure 8. Figure 8a presents the correlations between spectral ordinates of oscillators having the same damping ratio, which is set at 1%, 5%, and 20%. Figure 8b shows the correlations between spectral ordinates for the cases in which one of the oscillators has a fixed damping ratio of $\xi_2 = 1\%$ and a fixed period of $T_2 = 0.1$ s or $T_2 = 2$ s, whereas the period of vibration of the other oscillator is varied between $T_1 = 0.01$ and $T_1 = 10$ s and its damping ratios is set to $\xi_1 = 1\%$, $\xi_1 = 5\%$, and $\xi_1 = 20\%$. The differences between computed correlations and the regression model are negligible, and in most cases, the dashed lines representing the regression model cannot be distinguished from the solid lines representing the correlations obtained from the spectral accelerations computed using the set of ground motion records.

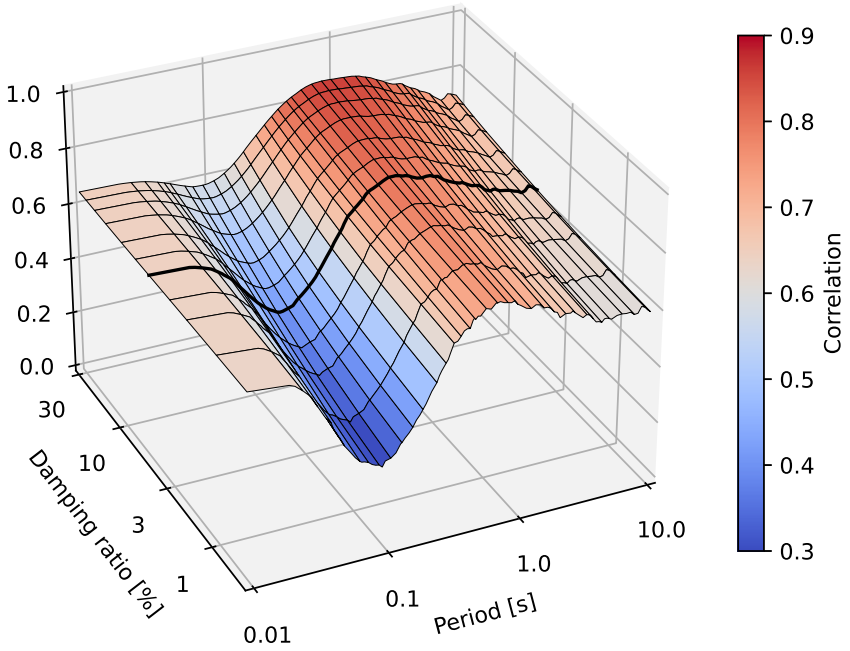

FIGURE 7 Correlations between PGV and spectral acceleration ordinates at different periods and different damping ratios. The thick black line corresponds to cases with 5% damping.

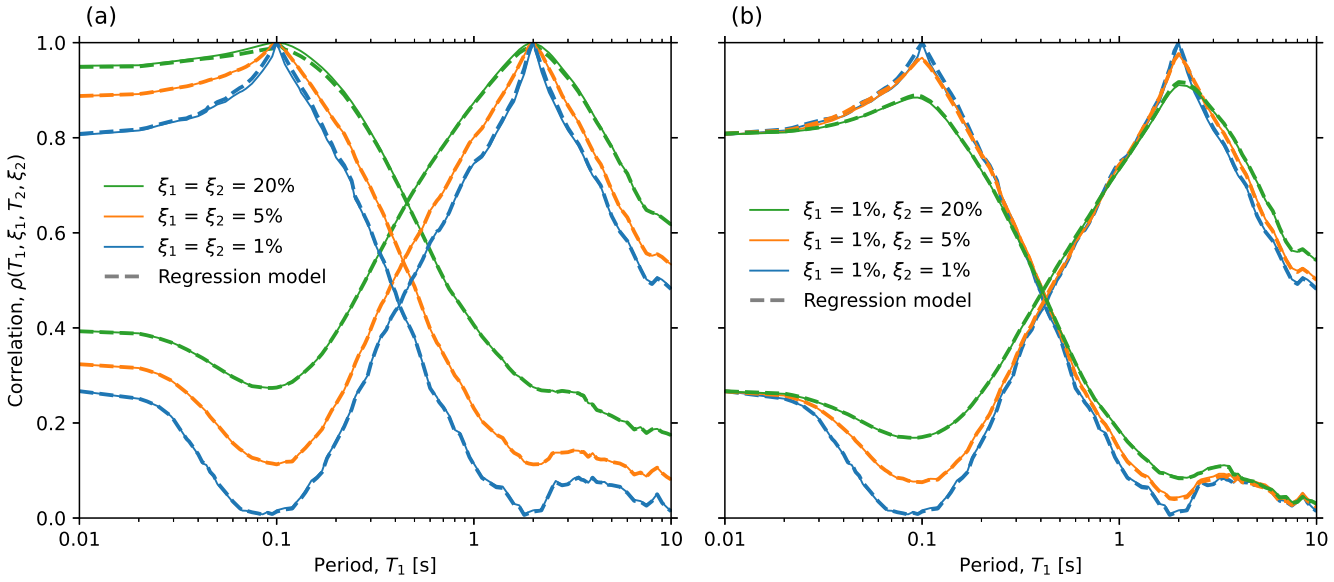

FIGURE 8 Comparison between the empirically-computed correlations (solid lines) and the regression model (dashed lines) proposed in this study for the cases when oscillators have different periods and have (a) the same damping ratio and (b) different damping ratios.

4 | IMPLICATIONS FOR CONDITIONAL SPECTRA

One common application of correlation models of spectral acceleration ordinates is the construction of conditional spectra, which provides a probabilistic description of the response spectra conditioned on the occurrence of given spectral acceleration at a period of interest.[16] The conditional logarithmic spectral acceleration at every period is assumed to follow a normal distribution with the following mean and standard deviation:

$$\mu_{\ln Sa(T)|\ln Sa(T^*)}(\xi) = \mu_{\ln Sa}(T,\xi) + \rho(T,\xi,T^*,\xi)\varepsilon(T^*)\sigma_{\ln Sa}(T,\xi) \tag{16}$$

$$\sigma_{\ln Sa(T)|\ln Sa(T^*)}(\xi) = \sigma_{\ln Sa}(T,\xi)\sqrt{1-\rho^2(T,\xi,T^*,\xi)} \tag{17}$$

where $\varepsilon(T^*)$ is the number of standard deviations by which the $\ln Sa(T^*)$ used for conditioning differs from the mean value predicted by a GMM. The computation of conditional spectra requires a GMM to estimate the logarithmic mean and standard deviation of spectral accelerations at all other periods (i.e., $\mu_{\ln Sa}$ and $\sigma_{\ln Sa}$, respectively), and a correlation model for spectral accelerations at different periods. To construct conditional spectra for damping ratios other than 5%, we can start with a GMM for 5%-damped spectral accelerations and compute the logarithmic mean and standard deviation with Equations (2) and (3) using a model for damping scaling. Then, the correlations between non-5%-damped spectral accelerations can be obtained from the results of this study. In the absence of these correlations, one option could be to use the correlations for the 5%-damped case:

$$\tilde{\mu}_{\ln Sa(T)|\ln Sa(T^*)}(\xi) = \mu_{\ln Sa}(T,\xi) + \rho_{5\%}(T,T^*)\varepsilon(T^*)\sigma_{\ln Sa}(T,\xi) \tag{18}$$

$$\tilde{\sigma}_{\ln Sa(T)|\ln Sa(T^*)}(\xi) = \sigma_{\ln Sa}(T,\xi)\sqrt{1-\rho_{5\%}(T,T^*)} \tag{19}$$

The implications of this simplifying assumption are illustrated in Figure 9 for response spectra of 1% and 30% damping using an example earthquake scenario. The example earthquake originates from a strike-slip fault and has a magnitude of 7, the Joyner-Boore and rupture distances are both 15 km, and the site has an average shear wave velocity in the top 30 m of soil of 700 m/s. Moreover, the conditioning period is 0.4 s and the conditioning spectral accelerations at this period satisfy $\varepsilon(T^*) = 1$ for both damping ratios. The computations used the GMM developed by Boore et al.[2] and the damping scaling factor model developed by Rezaeian et al.[13] For the 1% damping case, using the 5%-damped correlations overestimates the conditional mean spectrum (CMS) and underestimates the conditional standard deviation, whereas for the 30% damping case the CMS is underestimated and the conditional standard deviation is overestimated. The accuracy of using the 5%-damped correlations to estimate the CMS depends on the period of vibration, with the maximum differences in response spectral ordinates being approximately 10.0% for the 1%-damped CMS and 11.9% for the 30%-damped CMS, and occur at periods of approximately 0.07 to 0.1 s, respectively.

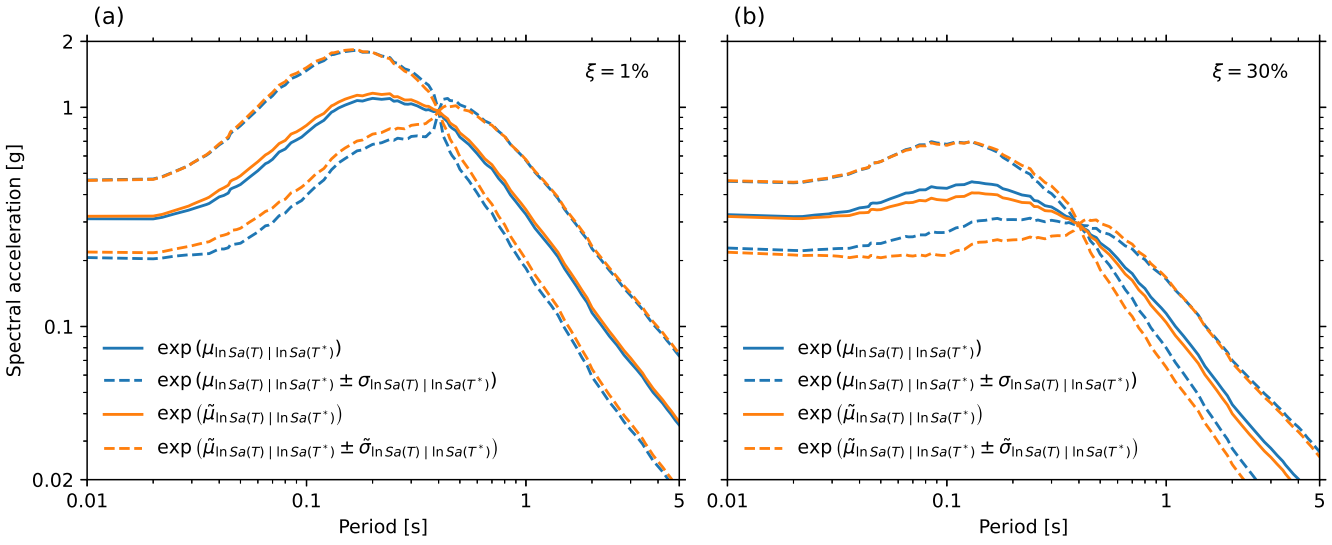

FIGURE 9 Conditional spectra for a conditioning period of 0.4 s and damping ratios of (a) $\xi = 1\%$ and (b) $\xi = 30\%$.

The same conditional spectra shown in Figure 9 were computed for all other damping ratios considered in this study using the same two options of correlation (i.e., 5%-damped correlations and the correlations of this study). The implications of using a 5%-damped correlation for all damping ratios are summarized in Figure 10 in terms of ratios of the conditional median spectral ordinates and ratios of the conditional logarithmic standard deviation. The results of Figure 10a show that the trends observed in Figure 9 can be extended to the rest of the damping ratios, i.e. using the 5%-damped correlations instead of the true correlation overestimates the conditional median spectral ordinates for damping ratios lower than 5%, and underestimates it for damping ratios higher than 5%. Conversely, Figure 10b shows that using 5%-damped correlations underestimates the conditional logarithmic standard deviation for damping ratios lower than 5% and overestimates it for damping ratios higher than 5%. Note that in the case of the ratios between the logarithmic standard deviations, the ratios are not shown for the conditioning period as they are indeterminate because the denominator is zero given that, by definition, there is no variability of the conditional spectra at the conditioning period.

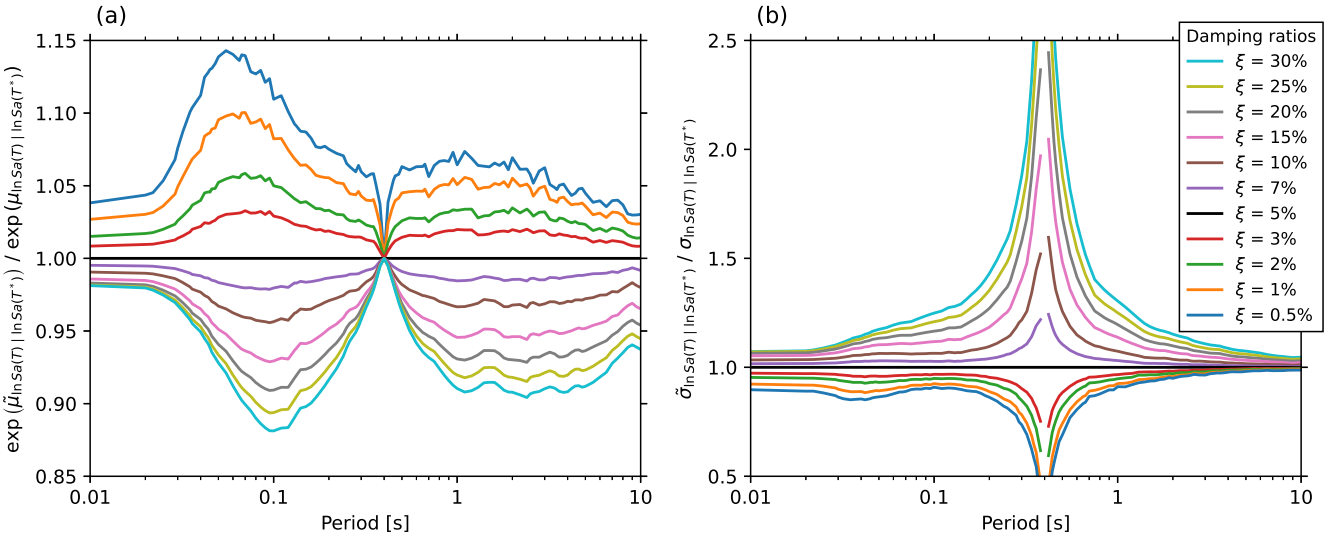

FIGURE 10 Ratios of (a) conditional median spectral ordinates and (b) conditional logarithmic standard deviations between the cases that consider 5%-damped correlations and the true correlations for the case in which the conditioning period is $T^* = 0.4$ s.

5 | CONCLUSIONS

This study evaluates the effect of damping ratio on the correlation between spectral acceleration ordinates at different periods using recorded ground motions. The resulting correlations of 5%-damped spectral acceleration ordinates computed in this study are similar to those computed in previous studies. However, the use of different damping ratios changes the correlations significantly. If the two periods for which the spectral accelerations are computed have the same damping ratio, their correlation increases as the damping ratio increases. For example, the correlation between spectral acceleration ordinates at 0.1 s and 1 s, which is approximately 0.23 for a damping ratio of 5%, is approximately 0.11 and 0.47 for damping ratios of 1% and 30%, respectively. When the two oscillators have different damping ratios, their correlations usually increase if any of the two damping ratios increase, provided that both periods are sufficiently separated from each other.

A nonlinear regression model was calibrated by using the correlations obtained from spectral accelerations computed from the ground motion records. The inputs of this model are the periods and damping ratios of the two oscillators for which the spectral accelerations are being estimated, and it is a generalization of previous models that only depend on the periods. The proposed regression model gives correlations that are almost identical to those computed with the ground motion records.

Several modeling decisions and assumptions must be made to compute correlations between spectral accelerations, such as the criteria to select ground motion records, the GMM, and the model used to modify spectral accelerations by damping (e.g.,

damping scaling factors). The effect of the GMM on the correlations was studied by using four different models, which resulted in different correlations, although, for most practical applications, it may be reasonable to neglect this dependence. The record selection criteria were studied by using three different sets of records from the NGA-West2 database combined with using a single GMM and shows a small effect on the resulting correlations. The differences are expected to be larger if the ground motions are obtained from different databases, especially if the ground motion records correspond to different tectonic regimes.

The damping-dependent correlation presented in this work can be useful for several applications, especially when damping ratios other than 5% are of interest, such as for high-rise buildings and structures with seismic isolation or energy dissipation devices. To illustrate its use, conditional spectra for various damping ratios were computed for an example earthquake scenario. The results were compared to the conditional spectra that would result if the 5%-damped correlations were used. For damping ratios lower than 5%, this assumption results in overestimating the conditional mean spectrum and underestimating the conditional standard deviation. Conversely, the assumption underestimates the conditional mean spectrum and overestimates the conditional standard deviation for damping ratios higher than 5%.

ACKNOWLEDGMENTS

We thank the National Agency for Research and Development (ANID) / Doctorado Becas Chile / 2019-72200307 and the Nancy Grant Chamberlain Fellowship at Stanford University for sponsoring the doctoral studies of the first author. We also thank David Boore for providing the list of ground motion records that were used to develop the Boore et al. GMM[2] and Jack Baker for helping us compare our results with the correlation model developed by Baker and Bradley[22].

DATA AVAILABILITY STATEMENT

The ground motion data used in this study was obtained from the NGA-West2 database flatfiles developed by the Pacific Earthquake Engineering Research Center (https://peer.berkeley.edu/research/data-sciences/databases, last accessed March 2021). The Python codes used to develop the proposed correlation model are available at the following Github repository: https://github.com/ajpoulos/Sa-correlations.

References

1. American Society of Civil Engineers . *Minimum design loads and associated criteria for buildings and other structures (ASCE/SEI 7-16)*. Reston, VA: American Society of Civil Engineers . 2016.

2. Boore DM, Stewart JP, Seyhan E, Atkinson GM. NGA-West2 equations for predicting PGA, PGV, and 5% damped PSA for shallow crustal earthquakes. *Earthquake Spectra* 2014; 30(3): 1057–1085.

3. Campbell KW, Bozorgnia Y. NGA-West2 ground motion model for the average horizontal components of PGA, PGV, and 5% damped linear acceleration response spectra. *Earthquake Spectra* 2014; 30(3): 1087–1115.

4. Chiou BSJ, Youngs RR. Update of the Chiou and Youngs NGA model for the average horizontal component of peak ground motion and response spectra. *Earthquake Spectra* 2014; 30(3): 1117–1153.

5. Çelebi M, Ghahari SF, Haddadi H, Taciroglu E. Response study of the tallest California building inferred from the Mw7. 1 Ridgecrest, California earthquake of 5 July 2019 and ambient motions. *Earthquake Spectra* 2020; 36(3): 1096–1118.

6. Cruz C, Miranda E. Insights into damping ratios in buildings. *Earthquake Engineering & Structural Dynamics* 2021; 50(3): 916–934.

7. Cruz C, Miranda E. Damping ratios of the first mode for the seismic analysis of buildings. *Journal of Structural Engineering* 2021; 147(1): 04020300.

8. Cruz C, Miranda E. Evaluation of the Rayleigh damping model for buildings. *Engineering Structures* 2017; 138: 324–336.

9. Trifunac MD, Lee VW. Empirical models for scaling pseudo relative velocity spectra of strong earthquake accelerations in terms of magnitude, distance, site intensity and recording site conditions. *Soil Dynamics and Earthquake Engineering* 1989; 8(3): 126–144.

10. Akkar S, Bommer JJ. Prediction of elastic displacement response spectra in Europe and the Middle East. *Earthquake Engineering & Structural Dynamics* 2007; 36(10): 1275–1301.

11. Newmark NM, Hall WJ. Earthquake spectra and design. Engineering Monographs on Earthquake Criteria, Structural Design, and Strong Motion Records, Earthquake Engineering Research Institute; El Cerrito, CA: 1982.

12. Lin YY, Chang KC. Study on damping reduction factor for buildings under earthquake ground motions. *Journal of Structural Engineering* 2003; 129(2): 206–214.

13. Rezaeian S, Bozorgnia Y, Idriss IM, Abrahamson N, Campbell K, Silva W. Damping scaling factors for elastic response spectra for shallow crustal earthquakes in active tectonic regions:"Average" horizontal component. *Earthquake Spectra* 2014; 30(2): 939–963.

14. Bazzuro P. Vector-valued probabilistic seismic hazard analysis (VPSHA). In: Proceedings of the 7th US National Conference on Earthquake Engineering. Earthquake Engineering Research Institute; 2002; Boston, MA.

15. Abrahamson N, Al Atik L. Scenario spectra for design ground motions and risk calculation. In: 9th US National and 10th Canadian Conference on Earthquake Engineering. ; 2010; Toronto, Canada.

16. Baker JW. Conditional mean spectrum: Tool for ground-motion selection. *Journal of Structural Engineering* 2011; 137(3): 322–331.

17. Baker JW, Cornell CA. Correlation of response spectral values for multicomponent ground motions. *Bulletin of the seismological Society of America* 2006; 96(1): 215–227.

18. Jayaram N, Baker JW. Statistical tests of the joint distribution of spectral acceleration values. *Bulletin of the Seismological Society of America* 2008; 98(5): 2231–2243.

19. Inoue T, Cornell CA. Seismic hazard analysis of multi-degree-of-freedom structures. Report No. RMS-8, Blume Earthquake Engineering Center; Stanford, CA: 1990.

20. Baker JW, Jayaram N. Correlation of spectral acceleration values from NGA ground motion models. *Earthquake Spectra* 2008; 24(1): 299–317.

21. Akkar S, Sandıkkaya MA, Ay BÖ. Compatible ground-motion prediction equations for damping scaling factors and vertical-to-horizontal spectral amplitude ratios for the broader Europe region. *Bulletin of Earthquake Engineering* 2014; 12(1): 517–547.

22. Baker JW, Bradley BA. Intensity measure correlations observed in the NGA-West2 database, and dependence of correlations on rupture and site parameters. *Earthquake Spectra* 2017; 33(1): 145–156.

23. Kotha SR, Bindi D, Cotton F. Site-corrected magnitude-and region-dependent correlations of horizontal peak spectral amplitudes. *Earthquake Spectra* 2017; 33(4): 1415–1432.

24. Ancheta TD, Darragh RB, Stewart JP, et al. NGA-West2 database. *Earthquake Spectra* 2014; 30(3): 989–1005.

25. Abrahamson NA, Silva WJ, Kamai R. Summary of the ASK14 ground motion relation for active crustal regions. *Earthquake Spectra* 2014; 30(3): 1025–1055.

26. Rezaeian S, Bozorgnia Y, Idriss IM, Campbell K, Abrahamson N, Silva W. Spectral damping scaling factors for shallow crustal earthquakes in active tectonic regions. PEER Report 2012/01, Pacific Earthquake Engineering Research Center; Berkeley, California: 2012.

27. Abrahamson NA, Youngs RR. A stable algorithm for regression analyses using the random effects model. *Bulletin of the Seismological Society of America* 1992; 82(1): 505–510.

28. Moré JJ. The Levenberg-Marquardt algorithm: implementation and theory. In: Watson GA., ed. *Numerical analysis.* Lecture Notes in Mathematics. Springer. 1978 (pp. 105–116).

29. Chiou BSJ, Youngs RR. An NGA model for the average horizontal component of peak ground motion and response spectra. *Earthquake Spectra* 2008; 24(1): 173–215.

30. Baker J. NGAW2_correlations [Source code]. https://github.com/bakerjw/NGAW2_correlations; 2016. Accessed March, 2022.

How to cite this article: Poulos A, Miranda E. Damping-dependent correlations between response spectral ordinates. *Earthquake Engng Struct Dyn*. 2023;52:1078-1090. doi:10.1002/eqe.3803